The electro-thermal stability of tantalum relative to aluminum and titanium in cylindrical liner ablation experiments at 550 kA

Adam M. Steiner, Paul C. Campbell, David A. Yager-Elorriaga, Kyle R. Cochrane, Thomas R. Mattsson, Nicholas M. Jordan, Ryan D. McBride, Y. Y. Lau, and Ronald M. Gilgenbach

Citation: Physics of Plasmas **25**, 032701 (2018); doi: 10.1063/1.5012891
View online: https://doi.org/10.1063/1.5012891
View Table of Contents: http://aip.scitation.org/toc/php/25/3
Published by the American Institute of Physics

Articles you may be interested in

Direct-drive inertial confinement fusion: A review
Physics of Plasmas **22**, 110501 (2015); 10.1063/1.4934714

The effects of microstructure on propagation of laser-driven radiative heat waves in under-dense high-Z plasma
Physics of Plasmas **25**, 032702 (2018); 10.1063/1.5012523

Applied axial magnetic field effects on laboratory plasma jets: Density hollowing, field compression, and azimuthal rotation
Physics of Plasmas **24**, 122701 (2017); 10.1063/1.5003777

Magnetic plasma expulsion
Physics of Plasmas **25**, 012508 (2018); 10.1063/1.5006887

Editorial: Preface to the 25th Volume of Physics of Plasmas
Physics of Plasmas **25**, 010401 (2018); 10.1063/1.5021964

In-flight neutron spectra as an ICF diagnostic for implosion asymmetries
Physics of Plasmas **25**, 022705 (2018); 10.1063/1.5018108

The electro-thermal stability of tantalum relative to aluminum and titanium in cylindrical liner ablation experiments at 550 kA

Adam M. Steiner,[1,a)] Paul C. Campbell,[1] David A. Yager-Elorriaga,[1,b)] Kyle R. Cochrane,[2] Thomas R. Mattsson,[2] Nicholas M. Jordan,[1] Ryan D. McBride,[1] Y. Y. Lau,[1] and Ronald M. Gilgenbach[1]

[1]*Plasma, Pulsed Power and Microwave Laboratory, Nuclear Engineering and Radiological Sciences Department, University of Michigan, Ann Arbor, Michigan 48109-21041, USA*
[2]*Sandia National Laboratories, Albuquerque, New Mexico 87185, USA*

(Received 8 November 2017; accepted 3 February 2018; published online 1 March 2018)

Presented are the results from the liner ablation experiments conducted at 550 kA on the Michigan Accelerator for Inductive Z-Pinch Experiments. These experiments were performed to evaluate a hypothesis that the electrothermal instability (ETI) is responsible for the seeding of magnetohydrodynamic instabilities and that the cumulative growth of ETI is primarily dependent on the material-specific ratio of critical temperature to melting temperature. This ratio is lower in refractory metals (e.g., tantalum) than in non-refractory metals (e.g., aluminum or titanium). The experimental observations presented herein reveal that the plasma-vacuum interface is remarkably stable in tantalum liner ablations. This stability is particularly evident when contrasted with the observations from aluminum and titanium experiments. These results are important to various programs in pulsed-power-driven plasma physics that depend on liner implosion stability. Examples include the magnetized liner inertial fusion (MagLIF) program and the cylindrical dynamic material properties program at Sandia National Laboratories, where liner experiments are conducted on the 27-MA Z facility. *Published by AIP Publishing*. https://doi.org/10.1063/1.5012891

I. INTRODUCTION

The ablation and implosion of cylindrical liners has been an important field of study within pulsed-power-driven plasma physics due to applications in dynamic material properties,[1,2] intense radiation generation,[3–6] and magnetized liner inertial fusion (MagLIF).[7–11] Recent MagLIF experiments have demonstrated fusion-relevant plasma conditions.[11,12] On a proposed larger current driver[13] MagLIF could one day provide a controlled high-yield fusion source (>1 MJ).[14] One of the factors that could potentially limit MagLIF performance is implosion asymmetry due to magnetohydrodynamic instabilities, including the magneto-Rayleigh-Taylor (MRT) instability. While the primary surface perturbation from which MRT grows is not yet fully understood, theoretical and experimental studies have supported the theory that the perturbation grows from the striation form of the electrothermal instability (ETI).[12,15–18]

ETI describes the exponential growth of a temperature perturbation in a medium that is ohmically heated and has a temperature-dependent electrical resistivity, $\eta(T)$. When resistivity increases with temperature, as in condensed metals, ETI tends to form striations perpendicular to the direction of current flow that ablate before the bulk material; it is believed that these ablated regions of the liner set the initial interface perturbation that seeds the subsequent development of MHD instabilities in liner implosions.

Additionally, a filamentation form of ETI exists, with perturbations developing parallel to the current flow; this form occurs in materials for which the resistivity decreases with temperature (e.g., plasma). Derivations of dispersion relations for both forms of ETI are available in other publications.[15,19]

Neglecting material expansion, the *instantaneous* growth rate of the striation-form of ETI is given by[15]

$$\gamma(t,T,k) = \frac{\frac{\partial \eta}{\partial T} J^2 - k^2 \kappa}{\rho c_p}, \tag{1}$$

where J is the time-dependent current density, k is the wavenumber of the perturbation, and κ, ρ, and c_p are the temperature-dependent thermal conductivity, mass density, and specific heat capacity of the current-carrying material, respectively. Following Oreshkin,[20] it is useful to define an explosion time τ_{ex}, which is the time when the liner completely vaporizes and begins to expand rapidly. For large pulsed-power machines capable of generating current densities of order 10^{13} A/cm^2, the magnetic pressure at the surface of the liner is generally high enough to prevent this explosion from occurring until after the material reaches the critical temperature T_{crit}.[20] Above T_{crit}, the liquid phase cannot exist regardless of pressure. With τ_{ex}, the *cumulative* ETI growth can be written as

$$\Gamma(k) = \int_0^{\tau_{ex}} \gamma(t, T(t), k) dt. \tag{2}$$

The physical meaning of $\Gamma(k)$ is *the number of e-foldings of a temperature perturbation* on the liner surface. This quantity determines how much faster a "hot" section of the liner reaches the point of ablation relative to the bulk liner

[a)]Now with Lockheed Martin Aeronautics, Palmdale, CA 93599, USA.
[b)]Now with Sandia National Laboratories, Albuquerque, NM 87135, USA.

material. By the time the bulk material has ablated, the hot sections have already expanded a certain distance that defines the initial interface perturbation for the subsequent evolution of MHD instabilities.

Taking the assumptions of: (1) a stationary material-vacuum interface prior to τ_{ex}; (2) a constant action integral[21] $h = \int_0^{\tau_{ex}} J^2 dt$; and (3) the fast explosion mode (defined such that the time to ablation is faster than the e-folding time for the m = 0 sausage instability, but much slower than the magnetic diffusion time), Oreshkin[20] derived an approximate expression for the cumulative growth of the fastest growing ETI mode

$$\Gamma_m = \Gamma(0) = \ln\left(\frac{T_{crit}}{T_{melt}}\right). \tag{3}$$

This surprising result indicates that the cumulative growth of the fastest growing ETI mode (and therefore the amplitude of the initial interface perturbation caused by ETI) depends only on the critical temperature and melting temperature of the liner material. Refractory metals (metals known for their high resistance to heat and wear, specifically tungsten, molybdenum, tantalum, niobium, and rhenium) tend to have low ratios of T_{crit}/T_{melt}. This theory predicts that such refractory metals should exhibit smaller interface perturbations at the point of explosion when compared to non-refractory metals (e.g., aluminum and titanium) driven by the same electrical current. Late-time plasma instabilities that grow from this ETI-generated interface perturbation are therefore expected to be smaller in amplitude for tantalum liners compared with non-refractory metals.

In this article, experimental results are presented that demonstrate the stability of tantalum liner ablations relative to aluminum and titanium. In Sec. II, the experimental setup is described. In Sec. III, the experimental results are presented, revealing the remarkable stability of an ablating tantalum liner compared with aluminum and titanium. It is also observed that the titanium liner exhibits lower cumulative growth compared with aluminum, a somewhat surprising result. These findings are discussed in Sec. IV, and they are summarized with our conclusions in Sec. V.

II. EXPERIMENTAL CONFIGURATION

Ablations of initially solid, thin-foil liners were performed on the Michigan Accelerator for Inductive Z-Pinch Experiments (MAIZE), a 1-MA linear transformer driver described in detail in Refs. 22–24. Foils of aluminum, titanium, and tantalum of thicknesses 3.0 μm, 2.0 μm, and 500 nm, respectively, were wrapped into a cylindrical geometry following the liner fabrication process described in Ref. 25. Strips of each foil material, measuring 2.1 cm wide by 1.5 cm tall, were wrapped around an insulating, dumbbell-shaped support structure of total length 3.4 cm and diameter 6.4 mm to form the liner targets (see Fig. 1). A single layer of aluminum tape (0.1 mm thick) was wrapped around the top 1.0 cm and bottom 1.4 cm of each support structure, providing a conducting path from the foil to the anode and cathode of the pulsed power hardware.

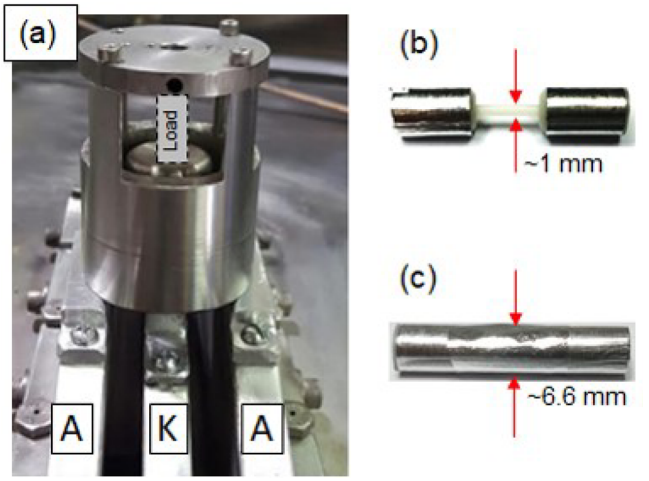

FIG. 1. (a) Closeup view of MAIZE load region showing the transition from tri-plate transmission line (with anode and cathode A, K) to coaxial load hardware adapter. The liner load acts as the center conductor for the coaxial transmission line and is situated in the load region. (b) Liner "dumbbell" support structure prior to applying the foil load (c) Support structure with 2.1 cm × 1.5 cm × 3.0 μm aluminum foil wrapped cylindrically to form a liner.

The purity of the foils used in these experiments exceeded 99% (based on manufacturer specifications), and the foil thicknesses were chosen to mass match the liners (i.e., all of the liners had a linear mass density of 1.8 ± 0.1 mg/cm). This mass density exceeds the previously established 0.5 mg/cm maximum that MAIZE is capable of imploding (previous experimental studies on MAIZE utilized liners of 0.2 mg/cm to achieve substantial implosion velocities[26]). Nevertheless, the magnetic pressure obtained in these shots was sufficient to provide a nearly stationary plasma-vacuum interface. This allowed sausage- and kink-like instabilities to be observed, decoupled from the magneto-Rayleigh Taylor instability. Previous experiments on MAIZE[27] have shown that liner ablations exhibit the m = 0 mode most strongly in this configuration.

Diagnostics fielded on the liner implosion experiments included differential output B-dot current monitors[28] and visible imaging using a 12-frame intensified charge coupled device camera (ICCD) with 5 ns temporal resolution. The optical system for the fast framing camera consisted of a switchyard of lenses and mirrors[23] designed to image the load at a magnification of approximately unity through a line filter at 532 nm (FWHM of 1 nm). The spatial resolution of this optical system was approximately 75 μm, and the field of view was greater than 1 cm × 1 cm. On some shots, a 2-ns duration, frequency-doubled, 532-nm Nd:YAG laser pulse was used to backlight the load. The laser intensity was of the order of self-emission from the ablating liner plasma at 532 nm, generating images with simultaneous contributions from self-emission and visible shadowgraphy. To synchronize the laser with the 12 camera frames, a single 2-ns pulse is split into many collinear beams using a 3.05-m resonating cavity with two 95/5% beam splitters.[27] Because the beam splitting process diminishes the intensity of the backlighter on each successive image (by >5%), it was nontrivial to track the plasma-vacuum interface over the 12 frames

obtained on a single shot. For this reason, later shots did not use the laser backlighter; instead, they relied solely on self-emission imaging to locate the plasma-vacuum interface. This approach is reasonable based on our prior experience with aluminum liners, where over 50 shots of instability amplitude data were analyzed and demonstrated little difference between instability amplitudes calculated from self-emission images only and those obtained from self-emission combined with the backlighter.[29]

Figure 2 shows a typical current trace measured by the B-dot probes. Peak currents of around 550 kA occurred at approximately 250 ns. The shot-to-shot variation in peak current and rise time was less than 5% regardless of liner material. At around 350 ns, the B-dot response exhibits an unphysical, monotonically increasing current measurement. This event occurs around the same time of the zero crossing of voltage and is believed to be due to electron bombardment on the B-dot sensor. A model of liner implosions on MAIZE, developed in Ref. 24, gives a load current fall time of about 400 ns for these experiments, indicating a total current pulse length of approximately 650 ns.

III. EXPERIMENTAL RESULTS AND ANALYSIS

Figure 3 shows ablation dynamics from aluminum, titanium, and tantalum liner implosions. The tantalum shot utilized the laser shadowgraphy backlighter, while the other shots show self-emission only. Contrast enhancement has been applied to the self-emission images and to the last frame of the tantalum shot to increase the visibility of the plasma-vacuum boundary. The large perturbations visible on the top and bottom of the ablating liner regions are due to the interface between the liner and the support structure. The dynamics of the aluminum and titanium shots appear qualitatively similar to the previous ablations of non-imploding liner loads on MAIZE,[27] with large, azimuthally correlated instability structures developing over 100 s of ns. By contrast, the tantalum shot demonstrates remarkable stability over the duration of the current pulse.

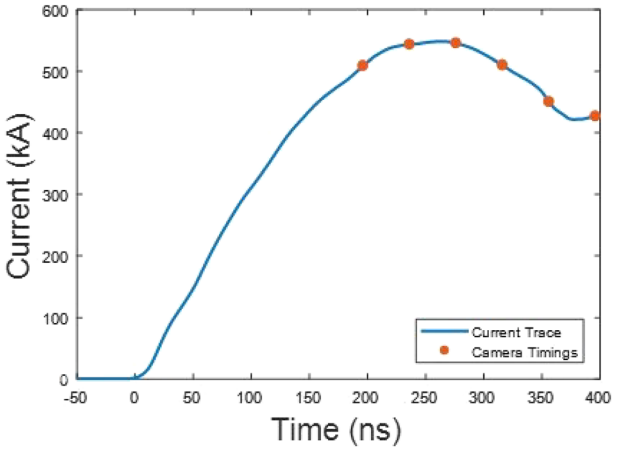

FIG. 2. Typical current measurement obtained by averaging four calibrated differential B-dot measurements taken in the radial transmission line of MAIZE.

In total, we conducted eight experiments with aluminum foils, six experiments with titanium foils, and three experiments with tantalum foils. Of these experiments, roughly half of them (four aluminum, three titanium, and two tantalum) used the dumbbell-shaped foil support structure described in Sec. II [see Fig. 1(b)], which resulted in a stationary plasma-vacuum interface for the duration of the experiments. By contrast, the remaining experiments tested a straight support structure that completely filled the interior of the cylindrical foil liner.[27] The straight support structure strictly prevents any radial implosion of the foil's plasma-vacuum interface, regardless of the foil mass used;[27] however, it also generates a back pressure that causes the foil's plasma-vacuum interface to accelerate radially outward. Regardless of the support structure used, the qualitative trends remained the same across all shots (i.e., the use of aluminum foils resulted in the largest instability structures, while the use of tantalum foils resulted in the smallest, nearly imperceptible, instability structures). Furthermore, the stationary-interface shots generally showed larger late-time instability structures than the outward exploding shots. This is expected because radially outward acceleration reduces the sausage instability growth rate.[30,31] In the case of a stationary plasma-vacuum interface, this growth rate reduction is absent for the sausage instability. To understand sausage mode growth without the complications of outward acceleration, the results presented in this paper are focused solely on the experiments that used the dumbbell-shaped support structure. Additionally, the experiments presented in Fig. 3 were chosen because: (1) their imaging times relative to the start-of-current were nearly identical; and (2) the entire span of the liner from the anode contact to the cathode contact was visible in the imaging field of view.

Each image was processed to find the location of the foil's plasma-vacuum interface (see Fig. 4). For each shot, a region of interest (ROI) was selected that excluded the large perturbations at the two ends of the liner, since these large perturbations have been attributed to increased local heating due to contact resistance.[32] The extracted ROIs were then rotated, and the interface was determined using an algorithm that searched for pixel values above a particular threshold value. Figure 4 shows a strong azimuthal correlation between the left and right plasma-vacuum boundaries, indicating the observed mode is the $m = 0$ sausage instability. With the position of the plasma-vacuum interface extracted from the image, the amplitude of the instability was then evaluated.

The time-dependent instability amplitude for the left and right interfaces of each image was determined using

$$A(t) = \sqrt{\frac{\sum_{i=1}^{N} (x_i - \bar{x})^2}{2N}}, \tag{4}$$

where x_i is the interface position at the ith data point on the interface function, $\bar{x}$ is the average interface position, and N is the number data points on each interface in the ROI. The left and right interface amplitudes were averaged for each image to give a measurement of instability amplitude at the time of the image.

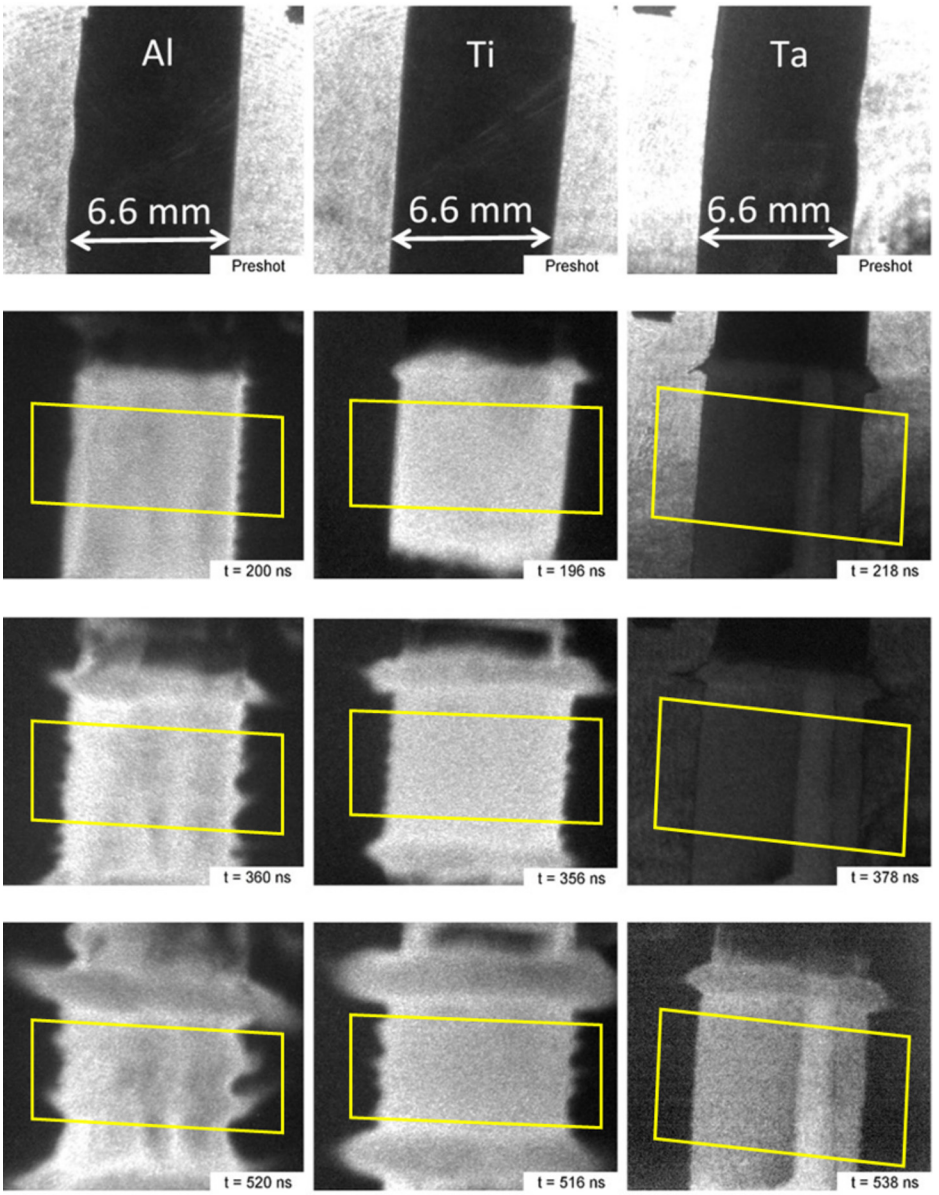

FIG. 3. Selected framing camera images from aluminum (left), titanium (center), and tantalum (right) liners, along with pre-shot shadowgraphs showing initial liner position. Self-emission images have been contrast enhanced to increase the visibility of the plasma-vacuum boundary. The boxes highlight the regions of interest (ROI) extracted for further analysis; these regions were chosen to exclude edge effects attributed to contact resistance. Note that the bright region in Ta images coincides with foil overlap intrinsic to the ultrathin liner wrapping method.

Figure 5 shows a plot of instability amplitude as a function of time for aluminum and titanium liners. An exponential growth function was fit to each shot to define an e-folding time. For aluminum, growth rate was found to be $5.4 \pm 0.7\ \mu s^{-1}$ (e-folding time 185 ± 25 ns), and for titanium, the growth rate was found to be $5.7 \pm 0.7\ \mu s^{-1}$ (e-folding time 175 ± 20 ns). For both materials, the measured instability amplitude was below the image resolution limit for early times, so only those amplitude data points which exceeded the resolution limit were used to fit the exponential.

The high degree of stability exhibited by the tantalum liner poses difficulties in analyzing the growth of instabilities, as all instability amplitudes extracted from the ROI fall below the image resolution threshold of 75 μm. We note that this observation held for all Ta liners tested, including both exploding and stationary-interface configurations. However, this does establish that the maximum instability amplitude at $t = 540$ ns (the time of the last available image) could not have exceeded the image resolution of 75 μm.

IV. DISCUSSION

For the sausage instability growth observed in the aluminum and titanium shots, the amplitude of the initial perturbation of the plasma-vacuum interface can be found. This initial perturbation is attributed to the end of the ETI phase, when the foil's surface first explodes, resulting in a rippled plasma-vacuum interface. (Note that the ETI growth phase begins when the foil melts and ends when the foil explodes.) To determine the initial perturbation amplitude, we extrapolate the exponential growth of the observed sausage instability backwards in time to the point when the foil's surface first explodes and the sausage growth begins. The explosion time is estimated by computing the action integral

$$h = \int_0^t j^2(t')dt' \tag{5}$$

and determining the time, t, when the action integral equals the tabulated values for the explosion of aluminum and

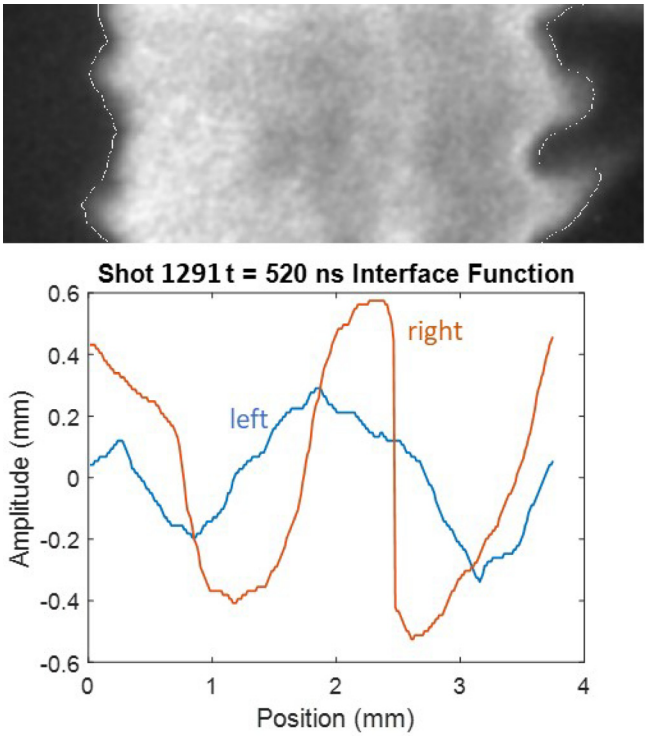

FIG. 4. (top) Region of interest from MAIZE Shot 1291 (3.0 μm aluminum liner) with the plasma-vacuum boundary fit highlighted in white. (bottom) Extracted interface function from the same shot showing interface amplitude as a function of axial position.

titanium, which are 1.8×10^9 A^{2}s/cm^4 and 1.1×10^9 A^{2}s/cm^4, respectively.[20,21]

For t $\lesssim$100 ns, the current rise is approximately linear with time and well characterized by the B-dot probes to within an accuracy of about 5%. Since the action integral is proportional to the time integral of current squared, and since the current rises approximately linearly with time up to the explosion time, the action integral goes approximately as t^3. Therefore, a departure from the tabulated action integral of explosion by as much as 50% changes the calculated explosion time by less than 10 ns. The 5% error of the B-dot probes adds an additional uncertainty of only $\pm$2 ns. Conservatively, we estimate the total error in the calculated explosion time to be $\pm$10 ns.

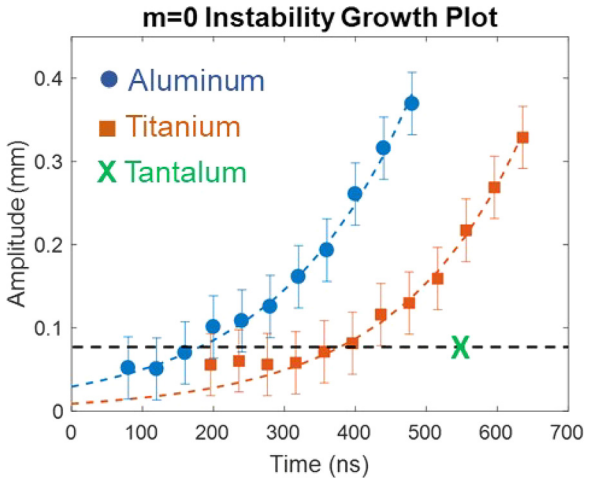

FIG. 5. Instability amplitude as a function of time for aluminum (blue circles) and titanium (red squares) with best-fit exponential functions for both materials shown in dashed lines. The dashed line at 0.075 mm represents the image resolution as measured by imaging an ASOFR resolution test chart. The green X represents the upper limit of the amplitude of the tantalum liner interface, equal to the resolution limit, at the latest available image time. Exponential fits to the aluminum and titanium data are used to estimate instability amplitudes at times prior to the development of features larger than the resolution limit.

For the shots depicted in Fig. 5, the aluminum liner reached the action of explosion at t = 56 ns ($\pm$10 ns), and the titanium liner reached the action of explosion at t = 54 ns ($\pm$10 ns). The measured exponential sausage growths depicted in Fig. 5 (e-folding times of 185 and 175 ns, respectively) were extrapolated backwards in time to these explosion times to yield initial perturbation amplitudes (i.e., to yield the initial sausage instability amplitudes right at the time of foil explosion). These explosion times yield initial amplitudes of 39 μm ($\pm$8 μm) for the aluminum ablation and 14 μm ($\pm$6 μm) for the titanium ablation. The uncertainty of these initial perturbation amplitudes accounts for the uncertainties from both calculated explosion time and growth rate fitting.

Because the perturbation amplitude on the tantalum shot never exceeds the image resolution, this analysis procedure cannot be applied. However, an upper bound on the initial interface amplitude can be determined given the upper bound imposed at 540 ns by the image resolution and assuming the growth of the m = 0 mode has a similar rate for the three materials. This assumption is supported by the aluminum and titanium data—the growth rate differs by only 5% between the two materials—and is believed to be reasonable for the following reasons: (1) the m = 0 instability grows as $1/\sqrt{\rho}$, where ρ is the density of the ablated plasma, in the case of no inward acceleration;[30] (2) the initial masses of the foils are equal (to within about 6%); and (3) the mean plasma-vacuum interface position is nearly stationary over hundreds of nanoseconds for all three materials. Taking this assumption and using the average growth rate observed from aluminum and titanium of 5.6 ± 0.7 μs^{-1}, we find that for an instability amplitude equal to the 75-μm image resolution at 540 ns, the initial amplitude at t = 50 ns ($\pm$10 ns) is at most 4.8 μm ($\pm$1 μm) for tantalum.

Oreshkin's study[20] reports a value of the ratio $R_T = \frac{T_{crit}}{T_{melt}}$ of 8.6 for aluminum. Other reported values of the critical temperature of aluminum are slightly lower, including an experimental measurement yielding $R_T = 6.1$ (Refs. 33–35) and calculation from Bushman-Lomonosov-Fortov (BLF) theory[35,36] yielding $R_T = 6.9$. Simulations by Desjarlais[37] using VASP (Vienna *ab initio* Simulation Program)[38] give $R_T = 6.4$ with a reported uncertainty of $\sim$10%. Tantalum is believed to have a substantially lower R_T: A theoretical calculation of critical temperature by Fortov *et al.*[39] yields $R_T = 4.1$ in tantalum. The most recently reported results known to the authors for a critical temperature of titanium are from calculations by Kerley,[40] which gives $R_T = 8.0$.

The R_T ratios using T_{crit} values reported in the literature predict that tantalum should have a lower cumulative ETI growth prior to explosion, and thus, tantalum should have a lower initial interface perturbation than aluminum, a

prediction that agrees with our experimental results. However, as the ratio for titanium is comparable with (or perhaps even higher than) that of aluminum, we would expect the titanium liner to show a larger initial interface perturbation to the aluminum liner, whereas the experimental measurement showed it to be a factor of ∼3 smaller. To investigate this surprising result further, simulations were performed in VASP[38] at Sandia National Laboratories to give updated estimates of the critical temperatures of tantalum and titanium. The VASP simulations gave $R_T = 3.8 \pm 0.3$ for tantalum, which is in good agreement with the Fortov calculation. However, the titanium VASP simulations yielded $R_T = 4.4 \pm 0.5$, a dramatically lower value than the previously reported result. These results are more in line with our experimental observations that the aluminum ablation was by far the most unstable; the titanium ablation was less unstable than aluminum; and the tantalum ablation was the most stable. We comment that the wide discrepancy in the computationally determined critical temperatures of various metals underscores the need for future experimental measurements of the critical temperatures.

In addition to R_T, the following three factors may contribute to the experimentally observed results:

1. The actual initial interface perturbation of the tantalum liner may be significantly lower than the upper bound of 4.8 μm, which would cause the separation between the cumulative ETI growth of tantalum and that of aluminum and titanium to be underrepresented. This proposed explanation could be investigated experimentally using a larger current density, which would increase the growth rate of the $m = 0$ mode and thus decrease the uncertainty on the initial amplitude.
2. The *surface resistivity* curves (where surface resistivity is the resistivity divided by the coefficient of volumetric expansion, the physically meaningful property for determining resistance of an *electrically thin* conductor) for titanium and tantalum are not monotonically increasing with temperature like that of most metals. Instead, they have a slight negative slope for a significant portion of the liquid phase.[41,42] This region of negative $\frac{\partial \eta}{\partial T}$ may be sufficient to smooth any azimuthally correlated surface perturbations that may have formed, causing a shift from $\Gamma_m = \frac{T_{crit}}{T_{melt}}$ to $\Gamma_m = \frac{T_{crit}}{T^*}$, where $T^* > T_{melt}$ is the temperature at which $\frac{\partial \eta}{\partial T}$ becomes positive again. This factor may warrant a future computational investigation.
3. The atomic number Z and/or the initial metal density ρ_{metal} may be an important factor, as the stability apparently increases with Z and/or ρ_{metal}.[43,44]

V. CONCLUSION

Ablation data were obtained from mass matched, initially solid foil liner experiments using aluminum, titanium, and tantalum. These data were used to calculate and compare the amplitude of the initial seed perturbation for MHD instabilities. It was hypothesized that the ETI was responsible for providing this initial seed and that the magnitude of the initial seed should be dependent on the ratio T_{crit}/T_{melt}. Tantalum, the material with the lowest such ratio, exhibited an extremely stable ablation—with an interface perturbation that was below the resolution threshold for the duration of the experiment—providing evidence to support the hypothesis. The weaker seeding of titanium compared with aluminum is surprising given their similar reported T_{crit}/T_{melt} ratios,[38–40] but this may be at least partially explained by the significantly lower value of T_{crit} calculated in VASP for titanium for this study. This latter result presents an interesting topic for future investigation.

ACKNOWLEDGMENTS

This research was supported by the DOE through Award No. DE-SC0012328, the NNSA under DOE Cooperative Agreement No. DE-NA0001984, Sandia National Laboratories Contract No. DE-NA0003525, and the National Science Foundation under Grant No. PHY-1705418. D.Y.E. was supported by an NSF fellowship under Grant No. DGE-1256260. The fast framing camera was supported by a DURIP, AFOSR Grant No. FA9550-15-1-0419. Sandia is a multimission laboratory managed and operated by National Technology and Engineering Solutions of Sandia, LLC., a wholly owned subsidiary of Honeywell International, Inc., for the U.S. Department of Energy's National Nuclear Security Administration under Contract No. DE-NA0003525.

[1]J. E. Bailey, G. A. Chandler, R. C. Mancini, S. A. Slutz, G. A. Rochau, M. Bump, T. J. Buris-Mog, G. Cooper, G. Dunham, I. Golovkin, J. D. Kilkenny, P. W. Lake, R. J. Leeper, R. Lemke, J. J. MacFarlane, T. A. Melhorn, T. C. Moore, T. J. Nash, A. Nikroo, D. S. Nielsen, K. L. Peterson, C. L. Ruiz, D. G. Schroen, D. Steinman, and W. Varnum, "Dynamic hohlraum radiation dynamics," Phys. Plasmas **13**(5), 056301 (2006).
[2]G. A. Rochau, "High performance capsule implosions driven by the Z-pinch dynamic hohlraum," Plasma Phys. Controlled Fusion **49**(12B), B591 (2007).
[3]M. D. Knudson, D. L. Hanson, J. E. Bailey, C. A. Hall, J. R. Asay, and C. Deeney, "Principal Hugoniot, reverberating wave, and mechanical reshock measurements of liquid deuterium to 400 GPa using plate impact techniques," Phys. Rev. B: Condens. Matter **69**, 144209 (2004).
[4]R. E. Reinovsky, "Instability growth in magnetically imploded high-conductivity cylindrical liners with material strength," IEEE Trans. Plasma Sci. **30**(5), 1764 (2002).
[5]J. E. Bailey, T. Nagayama, G. P. Loisel, G. A. Rochau, C. Blancard, J. Colgan, P. Cosse, G. Faussurier, C. J. Fontes, F. Gilleron, I. Golovkin, S. B. Hansen, C. A. Iglesias, D. P. Kilcrease, J. J. MacFarlane, R. C. Mancini, S. N. Nahar, C. Orban, J.-C. Pain, A. K. Pradhan, M. Sherrill, and B. G. Wilson, "A higher-than-predicted measurement of iron opacity at solar interior temperatures," Nature **517**, 56 (2015).
[6]M. R. Martin, R. W. Lemke, R. D. McBride, J. P. Davis, D. H. Dolan, M. D. Knudson, K. R. Cochrane, D. B. Sinars, I. C. Smith, M. Savage, W. A. Stygar, K. Killebrew, D. G. Flicker, and M. C. Herrmann, "Solid liner implosions on Z for producing multi-megabar, shockless compressions," Phys. Plasmas **19**(5), 056310 (2012).
[7]S. A. Slutz, M. C. Herrmann, R. A. Vesey, A. B. Sefkow, D. B. Sinars, D. C. Rovang, K. J. Peterson, and M. E. Cuneo, "Pulsed-power-driven cylindrical liner implosions of laser preheated fuel magnetized with an axial field," Phys. Plasmas **17**(5), 056303 (2010).
[8]S. A. Slutz and R. A. Vesey, "High-gain magnetized inertial fusion," Phys. Rev. Lett. **108**, 025003 (2012).
[9]M. E. Cuneo, M. C. Herrmann, D. B. Sinars, S. A. Slutz, W. A. Stygar, R. A. Vesey, A. B. Sefkow, G. A. Rochau, G. A. Chandler, J. E. Bailey, J. L. Porter, R. D. McBride, D. C. Rovang, M. G. Mazarakis, E. P. Yu, D. C. Lamppa, K. J. Peterson, C. Nakhleh, S. B. Hansen, A. J. Lopez, M. E.

Savage, C. A. Jennings, M. R. Martin, R. W. Lemke, B. W. Atherton, I. C. Smith, P. K. Rambo, M. Jones, M. R. Lopez, P. J. Christenson, M. A. Sweeney, B. Jones, L. A. McPherson, E. Harding, M. R. Gomez, P. F. Knapp, T. J. Awe, R. J. Leeper, C. L. Ruiz, G. W. Cooper, K. D. Hahn, J. McKenney, A. C. Owen, G. R. McKee, G. T. Leifeste, D. J. Ampleford, E. M. Waisman, A. Harvey-Thompson, R. J. Kaye, M. H. Hess, S. E. Rosenthal, and M. K. Matzen, "Magnetically driven implosions for inertial confinement fusion at Sandia National Laboratories," IEEE Trans. Plasma Sci. **40**(12), 3222 (2012).

[10]A. B. Sefkow, S. A. Slutz, J. Koning, M. M. Marinak, K. J. Peterson, D. B. Sinars, and R. A. Vesey, "Design of magnetized liner inertial fusion experiments using the Z facility," Phys. Plasmas **21**(7), 072711 (2014).

[11]M. R. Gomez, S. A. Slutz, A. B. Sefkow, D. B. Sinars, K. D. Hahn, S. B. Hansen, E. C. Harding, P. F. Knapp, P. F. Schmit, C. A. Jennings, T. J. Awe, M. Geissel, D. C. Rovang, G. A. Chandler, G. W. Cooper, M. E. Cuneo, A. J. Harvey-Thompson, M. C. Herrmann, M. H. Hess, O. Johns, D. C. Lamppa, M. R. Martin, R. D. McBride, K. J. Peterson, J. L. Porter, G. K. Robertson, G. A. Rochau, C. L. Ruiz, M. E. Savage, I. C. Smith, W. A. Stygar, and R. A. Vesey, "Experimental demonstration of fusion-relevant conditions in magnetized liner inertial fusion," Phys. Rev. Lett. **113**, 155003 (2014).

[12]T. J. Awe, K. J. Peterson, E. P. Yu, R. D. McBride, D. B. Sinars, M. R. Gomez, C. A. Jennings, M. R. Martin, S. E. Rosenthal, D. G. Schroen, A. B. Sefkow, S. A. Slutz, K. Tomlinson, and R. A. Vesey, "Experimental demonstration of the stabilizing effect of dielectric coatings on magnetically accelerated imploding metallic liners," Phys. Rev. Lett. **116**, 065001 (2016).

[13]W. A. Stygar, T. J. Awe, J. E. Bailey, N. L. Bennett, E. W. Breden, E. M. Campbell, R. E. Clark, R. A. Cooper, M. E. Cuneo, J. B. Ennis, D. L. Fehl, T. C. Genomi, M. R. Gomez, G. W. Greiser, F. R. Gruner, M. C. Herrmann, B. T. Hutsel, C. A. Jennings, D. O. Jobe, B. M. Jones, M. C. Jones, P. A. Jones, P. F. Knapp, J. S. Lash, K. R. Lechien, J. J. Leckbee, R. J. Leeper, S. A. Lewis, F. W. Long, D. j. Lucero, E. A. Madrid, M. R. Martin, M. K. Matzen, M. G. Mazarakis, R. D. McBride, G. R. Mckee, C. L. Miller, J. K. Moore, C. B. Mostrom, T. D. Mulville, K. J. Peterson, J. L. Porter, D. B. Reisman, G. A. Rochau, D. V. Rose, D. C. Rovang, M. E. Savage, M. E. Sceiford, P. F. Schmit, R. F. Schneider, J. Schwarz, A. B. Sefkow, D. B. Sinars, S. A. Slutz, R. B. Spielman, B. S. Stoltzfus, C. Thoma, R. A. Vesey, P. E. Wakeland, D. R. Welch, M. L. Wisher, and J. R. Woodworth, "Conceptual designs of two petawatt-class pulsed-power accelerators for high-energy-density-physics experiments," Phys. Rev. Accel. Beams **18**, 110401 (2015).

[14]S. A. Slutz, W. A. Stygar, M. R. Gomez, K. J. Peterson, A. B. Sefkow, D. B. Sinars, R. A. Vesey, M. Campbell, and R. Betti, "Scaling magnetized liner inertial fusion on Z and future pulsed-power accelerators," Phys. Plasmas **23**, 022702 (2016).

[15]K. J. Peterson, D. B. Sinars, E. P. Yu, M. C. Herrmann, M. E. Cuneo, S. A. Slutz, I. C. Smith, B. W. Atherton, M. D. Knudson, and C. Nakhleh, "Electrothermal instability growth in magnetically driven pulsed power liners," Phys. Plasmas **19**, 092701 (2012).

[16]K. J. Peterson, E. P. Yu, D. B. Sinars, M. E. Cuneo, S. A. Slutz, J. M. Koning, M. M. Marinak, C. Nakhleh, and M. C. Herrmann, "Simulations of electrothermal instability growth in solid aluminum rods," Phys. Plasmas **20**, 056305 (2013).

[17]K. J. Peterson, T. J. Awe, E. P. Yu, D. B. Sinars, E. S. Field, M. E. Cuneo, M. C. Herrmann, M. Savage, D. G. Schroen, K. Tomlinson, and C. Nakhleh, "Electrothermal instability mitigation by using thick dielectric coatings on magnetically imploded conductors," Phys. Rev. Lett. **112**, 135002 (2014).

[18]T. J. Awe, E. P. Yu, K. C. Yates, W. G. Yelton, B. S. Bauer, T. M. Hutchinson, S. Fuelling, and B. B. Mckenzie, "On the evolution from micrometer-scale inhomogeneity to global overheated structure during the intense joule heating of a Z-pinch rod," IEEE Trans. Plasma Sci. **45**(4), 584 (2017).

[19]D. D. Ryutov, M. S. Derzon, and M. K. Matzen, "The physics of fast Z pinches," Rev. Mod. Phys. **72**(1), 167 (2000).

[20]V. I. Oreshkin, "Thermal instability during an electrical wire explosion," Phys. Plasmas **15**, 092103 (2008).

[21]G. A. Mesyats, *Cathode Phenomena in a Vacuum Discharge: The Breakdown, the Spark, and the Arc* (Nauka, Moscow, 2000).

[22]R. M. Gilgenbach, M. R. Gomez, J. C. Zier, W. W. Tang, D. M. French, Y. Y. Lau, M. G. Mazarakis, M. E. Cuneo, M. D. Johnston, B. V. Oliver, T. A. Melhorn, A. A. Kim, and V. A. Sinebryukhov, "MAIZE: A 1 MA LTD-driven Z-pinch at the University of Michigan," AIP Conf. Proc. **1088**, 259 (2009).

[23]J. C. Zier, R. M. Gilgenbach, D. A. Chalenski, Y. Y. Lau, D. M. French, M. R. Gomez, S. G. Patel, I. M. Rittersdorf, A. M. Steiner, M. Weis, P. Zhang, M. Mazarakis, M. E. Cuneo, and M. Lopez, "Magneto-Rayleigh_Taylor experiments on a MegaAmpere linear transformer driver," Phys. Plasmas **19**, 032701 (2012).

[24]A. M. Steiner, D. A. Yager-Elorriaga, S. G. Patel, N. M. Jordan, R. M. Gilgenbach, A. S. Safronova, V. L. Kantsyrev, V. V. Shlyaptseva, I. Shrestha, and M. T. Schmidt-Petersen, "Determination of plasma pinch time and effective current radius of double planar wire array implosions from current measurements on a 1-MA linear transformer driver," Phys. Plasmas **23**(10), 101206 (2016).

[25]D. A. Yager-Elorriaga, A. M. Steiner, S. G. Patel, N. M. Jordan, Y. Y. Lau, and R. M. Gilgenbach, "Technique for fabrication of ultrathin foils in cylindrical geometry for liner-plasma implosion experiments with sub-megaampere currents," Rev. Sci. Instrum. **86**, 113506 (2015).

[26]D. A. Yager-Elorriaga, P. Zhang, A. M. Steiner, N. M. Jordan, P. C. Campbell, Y. Y. Lau, and R. M. Gilgenbach, "Discrete helical modes in imploding and exploding cylindrical, magnetized liners," Phys. Plasmas **23**, 124502 (2016).

[27]D. A. Yager-Elorriaga, P. Zhang, A. M. Steiner, N. M. Jordan, Y. Y. Lau, and R. M. Gilgenbach, "Seeded and unseeded helical modes in magnetized, non-imploding cylindrical liner plasmas," Phys. Plasmas **23**, 101205 (2016).

[28]T. C. Wagoner, W. A. Stygar, H. C. Ives, T. L. Gilliland, R. B. Spielman, M. F. Johnson, P. G. Reynolds, J. K. Moore, R. L. Mourning, D. L. Fehl, K. E. Androlewicz, J. E. Bailey, R. S. Broyles, T. A. Dinwoodie, G. L. Donovan, M. E. Dudley, K. D. Hahn, A. A. Kim, J. R. Lee, R. J. Leeper, G. T. Leifeste, J. A. Melville, J. A. Mills, L. P. Mix, W. B. S. Moore, B. P. Peyton, J. L. Porter, G. A. Rochau, G. E. Rochau, M. E. Savage, J. F. Seamen, J. D. Serrano, A. W. Sharpe, R. W. Shoup, J. S. Slopek, C. S. Speas, K. W. Struve, D. M. VanDeValde, and R. M. Woodring, "Differential-output B-dot and D-dot monitors for current and voltage measurements on a 20-MA, 3-MV pulsed-power accelerator," Phys. Rev. Accel. Beams **11**, 100401 (2008).

[29]D. A. Yager-Elorriaga, Ph.D. dissertation, University of Michigan, Ann Arbor, 2017.

[30]M. R. Weis, P. Zhang, Y. Y. Lau, P. F. Schmidt, K. J. Peterson, M. Hess, and R. M. Gilgenbach, "Coupling of sausage, kink, and magneto-Rayleigh–Taylor instabilities in a cylindrical liner," Phys. Plasmas **22**, 032706 (2015).

[31]M. R. Weis, Ph.D. dissertation, University of Michgan, Ann Arbor, 2015.

[32]M. R. Gomez, D. M. French, W. Tang, P. Zhang, Y. Y. Lau, and R. M. Gilgenbach, "Experimental validation of a higher dimensional theory of electrical contact resistance," Appl. Phys. Lett. **95**, 072103 (2009).

[33]G. R. Gathers, "Thermophysical properties of liquid copper and aluminum," Int. J. Thermophys. **4**(3), 209 (1983).

[34]G. R. Gathers and M. Ross, "Properties of hot expanded liquid aluminum," J. Non-Cryst. Solids **61-62**, 59 (1984).

[35]P. Renaudin, C. Blancard, J. Clerouin, G. Fassurier, P. Noiret, and V. Recoules, "Aluminum equation-of-state data in the warm dense matter regime," Phys. Rev. Lett. **91**(7), 075002 (2003).

[36]A. V. Bushman, I. V. Lomonosov, and V. E. Fortov, *Equations of State of Metals at High Energy Densities* (Institute of Chemical Physics, Russian Academy of Sciences, Chernogolvka, 1992).

[37]M. P. Desjarlais, "Quantum molecular dynamics simulations for generating equation of state data," in *CP1161, Atomic Processes in Plasmas*, edited by K. B. Fournier (AIP, 2009).

[38]G. Kresse and J. Hafner, "*Ab initio* molecular dynamics for liquid metals," Phys. Rev. B **47**, 558 (1993).

[39]V. E. Fortov, K. V. Khishchenko, P. R. Levashov, and I. V. Lomonosov, "Wide-range multi-phase equations of state for metals," Nucl. Instrum. Methods Phys. Res. A **415**, 604 (1998).

[40]G. I. Kerley, "Equations of state for titanium and Ti6A14V alloy," Report No. SAND2003-3785, Sandia National Laboratories, Albuquerque, NM, 2003.

[41]H. Jager, W. Neff, and G. Pottlacher, "Improved thermophysical measurements on solid and liquid tantalum," Int. J. Thermophys. **13**(1), 83 (1992).

[42]G. R. Gathers, "Electrical resistivity and thermal expansion of liquid titanium and zirconium," Int. J. Thermophys. **4**(3), 271 (1983).

[43]F. J. Wessel, Hafiz-Ur-Rahman, P. Ney, and R. Presura, "Fusion in a staged Z-pinch," IEEE Trans. Plasma Sci. **43**(8), 2463 (2015).

[44]H. U. Rahman, F. J. Wessel, P. Ney, R. Presura, R. Ellahi, and P. K. Shukla, "Shock waves in a Z-pinch and the formation of high energy density plasma," Phys. Plasmas **19**, 122701 (2012).